Measurement of a linear Stark interference effect on the rubidium $D1$ absorption line

Xu Chen,* F. R. Huang-Hellinger,† B. R. Heckel, and E. N. Fortson
Department of Physics, FM-15, University of Washington, Seattle, Washington 98195
(Received 17 June 1994)

We have measured the magnetic dipole ($M1$) and electric quadrupole ($E2$) amplitudes in the $D1$ transition of rubidium atoms placed in a static electric field, $\vec{\mathcal{E}}_s$. The interference of the Stark induced $M1$ and $E2$ amplitudes with the normal $E1$ amplitude gives the atomic absorptivity a linear dependence on $\vec{\mathcal{E}}_s$ and on the atomic spin polarization. We find that the fractional change in absorptivity due to the Stark interference is $a_{M1} + a_{E2} = (-2.37 \pm 0.37 \pm 0.28) \times 10^{-8}$ (kV/cm)$^{-1}$.

PACS number(s): 32.60.+i, 42.50.Wm, 32.80.−t, 35.80.+s

INTRODUCTION

A familiar example of the Stark mixing of atomic states occurs when a weak magnetic-dipole ($M1$) transition acquires a Stark induced electric-dipole ($E1$) component, causing both the transition rate to increase and interesting interference effects to appear [1–4]. On the other hand, to our knowledge, the interference of Stark induced $M1$ and electric quadrupole ($E2$) components with an allowed $E1$ transition has never been observed, mostly due to the smallness of the effects in this case. As part of an effort to search for a permanent atomic electric-dipole moment, for which an atomic absorption signal linear in an applied electric field is ultimately detected, we were lead to investigate the Stark interference effects on an allowed $E1$ transition. We report here our measurement of the interference of Stark induced $M1$ and $E2$ amplitudes with the normal $E1$ amplitude in the $5S_{1/2}$-$5P_{1/2}$ $D1$ transition in atomic rubidium.

In a previous report [5], it was shown that in the presence of a static electric field, $\vec{\mathcal{E}}_s$, the fractional change in the absorptivity, α, of the $D1$ transition in alkali atoms is given by

$$\frac{\Delta\alpha}{\alpha} = (a_{M1} + a_{E2})(\hat{\epsilon} \cdot \vec{\mathcal{E}}_s)(\hat{k} \times \hat{\epsilon}) \cdot \vec{\sigma}, \qquad (1)$$

where $\hat{\epsilon}$ and $\hat{k}$ are unit vectors parallel to the optical electric field and propagation direction of the light, respectively, $\vec{\sigma}$ is the atomic spin polarization, and the coefficient $a_{M1} + a_{E2}$ is the amplitude of the linear Stark interference effect. A calculation of a similar effect in atomic mercury also has been carried out [6].

We have measured $a_{M1} + a_{E2}$ for the $D1$ line of atomic rubidium by monitoring the small change in absorption when $\vec{\mathcal{E}}_s$ was reversed. Our experimental result is

$$a_{M1} + a_{E2} = (-2.37 \pm 0.37 \pm 0.28) \times 10^{-8} \text{ (kV/cm)}^{-1}. \qquad (2)$$

The first error quoted is statistical and the second is systematic. The result is in good agreement with the prediction from atomic theory [5]: $a_{M1} + a_{E2} = -2.12 \times 10^{-8}$ (kV/cm)$^{-1}$

EXPERIMENTAL METHOD

A schematic diagram of the experimental apparatus is shown in Fig. 1. Rubidium vapor was contained in a quartz cell (labelled RB3 in Fig. 1) made from a 10 mm long section of 25×25 mm^2 tubing with platinum coated quartz plates glued to the ends with Torr-Seal epoxy. The cell was filled with 200 torr of nitrogen and a small amount of metallic Rb, and was centered inside of an oven. The oven was centered within three layers of magnetic shielding. The temperature of the oven was regulated to 80 °C during the experiment to provide an optical depth of ≈ 1.2 for $D1$ radiation. Three mutually perpendicular solenoids were mounted within the shields for magnetic field control.

To maximize the interference amplitude in Eq. (1), $\vec{\mathcal{E}}_s$ was applied along the (vertical) $\hat{x}$ axis, $\vec{\sigma}$ was oriented along $\hat{z}$, and $\hat{k}$ was along $-\hat{y}$. The linear polarization of the probe beam light, $\hat{\epsilon}$, was alternated between $\hat{x} \pm \hat{z}$. The coordinate system for our measurement is illustrated in Fig. 2.

Atomic polarization $\vec{\sigma}$ was created by optical pumping using the light from an $Al_xGa_{1-x}As$ semiconductor laser whose wavelength was locked to the 795 nm $F = 3$ hyperfine component of the ^{85}Rb $D1$ line. The laser pumping light, directed along $\hat{z}$, was first linearly polarized and then passed through a Pockels cell whose voltage was set to produce a retardation of $\pm\lambda/4$. The circular polarization of the pump beam light was reversed at 12 Hz by square wave modulation of the Pockels cell voltage. A relatively large magnetic field, $B_z \approx 5$ mG, was applied to maintain the direction of $\vec{\sigma}$. The pumping rate of $\vec{\sigma}$ was $\geq 10^3$ sec^{-1}.

A less intense $Al_xGa_{1-x}As$ diode laser, locked to the

*Present address: Microsoft Corporation, One Microsoft Way, Redmond, WA 98052.
†Present address: Department of Radiology, Massachusetts General Hospital, 55 Fruit St., Boston, MA 02114.

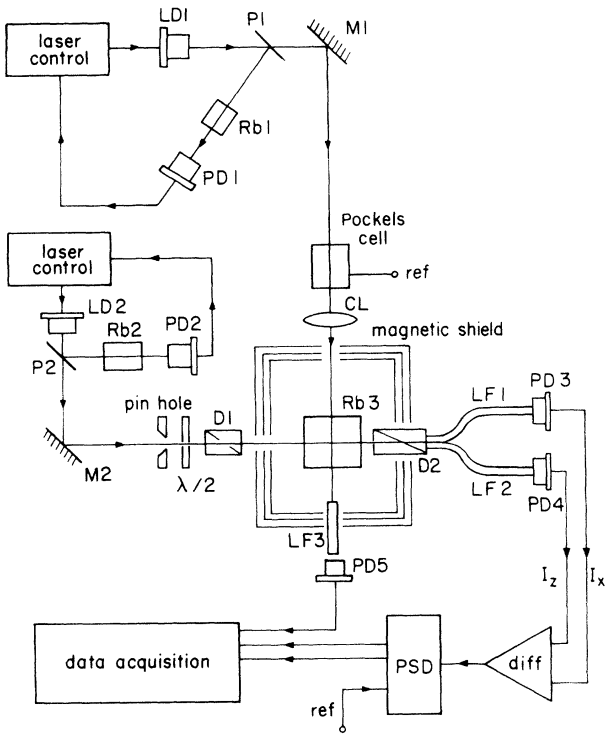

FIG. 1. Schematic view of the measurement apparatus. LD1 and LD2 are the pump and probe laser diodes, respectively; $P1$ and $P2$ are beam splitters; RB1 and RB2 are vacuum rubidium vapor cells used to lock the laser frequencies, RB3 is the buffered rubidium cell used for the interference measurement; PD1 through PD5 are photodiodes; $M1$ and $M2$ are mirrors; LF1, LF2, and LF3 are light fiber bundles; CL is a cylindrical lens; $D1$ and $D2$ are a Glan-Thompson and a Wollaston prism, respectively; and PSD is a phase sensitive detector.

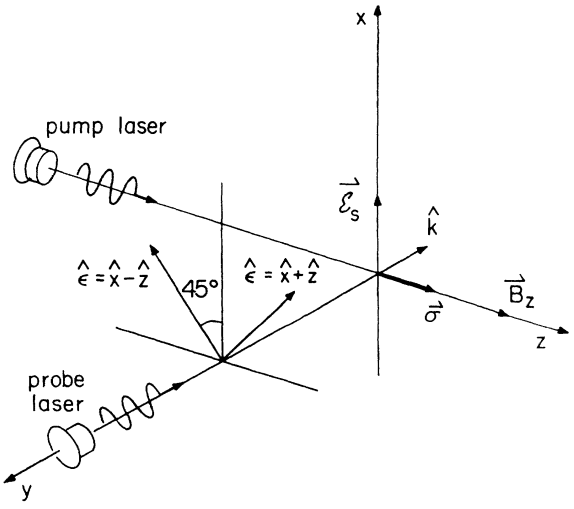

FIG. 2. Coordinate system for the interference measurement. The static electric field was applied along $\hat{x}$; the atomic polarization was created along $\pm\hat{z}$; the probe beam polarization was along $\hat{x} \pm \hat{z}$.

$F = 2$ to $F = 1$ hyperfine transition of the ^{87}Rb $D1$ line, was used to probe the Stark interference. The probe beam light was linearly polarized by a Glan-Thompson polarizer that was held in a rotary mount. Each day the polarizer would be rotated by 90° to provide the two directions for $\hat{\epsilon}$. A Wollaston crystal beam splitter was used to separate the $\hat{z}$ and $\hat{x}$ polarization components of the probe beam light that was transmitted through the vapor cell, so that the intensity of each component, I_z and I_x, was detected in separate photodetectors. From Eq. (1) it can be seen that the linear Stark interference occurs only for the $\hat{x}$ polarization component of the probe light. By taking $I_x - I_z$ to be the Stark interference signal, intensity noise of the probe beam was reduced by a factor of 6 compared to I_x alone. The signal, $I_x - I_z$, was phase detected at 12 Hz and the output of the phase detector was digitized at 0.5 Hz and stored by a computer for subsequent analysis.

Data was accumulated overnight: one run per night. During each run, $\hat{\epsilon}$ was constant while two high voltage supplies (one positive and one negative) were switched every 26 sec to produce an electric field across the vapor cells in a sequence $(+\mathcal{E}_s, 0, -\mathcal{E}_s, 0)\hat{z}$, with $\mathcal{E}_s = 3$ kV/cm. The first 10 sec of each 26 sec dwell was ignored to allow transient currents to decay. During the day, calibrations were performed and shorter runs were taken with a small B_y (≈ 0.3 mG) applied in addition to B_z. These shorter runs were used to measure potential systematic errors due to the quadratic Stark shift, to be discussed later. Each data set consisted of eight long (overnight) runs with eight associated short systematic test runs, four each with $\hat{\epsilon}$ along $\hat{x} \pm \hat{z}$. Between data sets, the Rb vapor cell would be removed to check the conductivity of the platinum electrodes (slowly corroded by the alkali). The cell would be remounted with its orientation rotated by 90°, and after four rotations, the cell would be flipped over and rotated four more times. Nine data sets were taken in all, eight for each orientation of one vapor cell, and the ninth using a different cell.

The 32 digitized values for each dwell of the electric field reversal sequence were averaged, and a string analysis performed on the averaged values to extract the signals linear, $S(\vec{\mathcal{E}}_s)$, and quadratic, $S(\mathcal{E}_s^2)$, in $\vec{\mathcal{E}}_s$. Weights of 1/8, −3/8, 3/8, and −1/8 were used on consecutive $+\mathcal{E}_s, -\mathcal{E}_s, +\mathcal{E}, -\mathcal{E}_s$ voltage dwells to obtain $S(\vec{\mathcal{E}}_s)$, while weights of −1/2, 1, and −1/2 were used on consecutive $0, \pm\mathcal{E}_s, 0$ voltage dwells to obtain $S(\mathcal{E}_s^2)$. The scatter of the string results was used to assign an error for each run.

CALIBRATION

The calibration of the sensitivity of the experiment requires the measurement of the absorptivity, α, of the Rb atoms at the wavelength of the probe light, the average atomic polarization, $\vec{\sigma}$, and the magnitude and direction of $\vec{\mathcal{E}}_s$. To determine α, the light intensity incident on the vapor cell, $I_{\rm inc}(\lambda)$, and the light intensity transmitted through the cell, $I(\lambda)$, were measured at three wavelengths: λ_0, the wavelength used for normal data taking,

and λ_a and λ_b, wavelengths well outside of the Rb absorption profile at either side of the $D1$ line. In addition, the fraction (11%) of nonresonant (off-mode) light when tuned to λ_0 was measured by placing a high density, high pressure Rb vapor cell in the beam path to absorb the resonant light. For these measurements, the probe light was linearly polarized and σ_y was held to zero by adjustment of B_y. The absorptivity is then found from the expression

$$I(\lambda_0) = I_0(\lambda_0)\left(0.89e^{-\alpha} - 0.11\right), \quad (3)$$

where $I_0(\lambda_0)$ is the transmitted light at λ_0 for no atoms in the cell, inferred from $I_{\rm inc}(\lambda_0, \lambda_a, \lambda_b)$ and $I(\lambda_a, \lambda_b)$. The absorptivities for each data set are listed in Table I.

The handedness of the pump beam circular polarization for each Pockels cell voltage was determined by use of a Michelson interferometer. Several times during each data set, $\langle\vec{\sigma}\rangle = \sigma\hat{z}$ was measured by using the relation

$$I(\lambda_0) = I_0(\lambda_0)\left(0.89e^{-\alpha(1-P_L\sigma_y)} - 0.11\right), \quad (4)$$

where P_L is the circular polarization of the probe beam. A zeroth order quarter wave retardation plate was inserted in the path of the probe beam to make $P_L \approx \pm 1$, while a field $B_y \approx 1$ mG was applied in addition to B_z to create a σ_y given by

$$\sigma_y = \sigma\cos\theta\sin\theta \quad (5)$$

where $\tan\theta = B_y/B_z$. The probe beam intensity was then measured for $P_L = \pm 1$ and for $\pm B_y$. From these measurements, σ_y and hence σ was determined. The results for σ are shown in Table I. The variation in σ between data sets was due to changes in the overlap of the pump and probe beam geometric profiles within the vapor cell as the cell was changed in orientation.

The average value of $\vec{\mathcal{E}}_s \cdot \hat{z}$ along the 10 mm length of the vapor cell was 3 kV/cm. We were unable to measure directly its value at the overlap region of the two laser beams within the cell. Instead, with the pump beam turned off, the probe beam was used to measure the quadratic Stark shift at applied voltages of 2, 3, 4, and 5 kV. If we assume that $\vec{\mathcal{E}}_s$ is given by (applied voltage)/10 mm, then our measurements correspond to an atomic polarizability at line center, $\alpha_E = (61 \pm 3) \times 10^{-24}$ cm^3, where the quadratic Stark shift is given by $\alpha_E\mathcal{E}_s^2/2$. This result is in good agreement with beam measurements of the polarizability [7]: $\alpha_E = (72 \pm 18) \times 10^{-24}$ cm^3. We conclude that the magnitude of $\vec{\mathcal{E}}_s$ at the cell center is at least 90% of the value given by (applied voltage)/10 mm. A possible small tilt in the direction of $\vec{\mathcal{E}}_s$ away from the $\hat{z}$ axis is of no consequence because it averages to zero upon reversal of the orientation of the cell.

SYSTEMATIC ERRORS

There were two potentially serious sources for systematic errors in our measurement: rotations of $\hat{\epsilon}$ about a residual σ_y, and imperfect cancellation of quadratic Stark shift effects. The real part of the atomic vapor index of refraction gives rise to optical rotation: a rotation of the linearly polarized $\hat{\epsilon}$ about $\hat{k}$ that is proportional to σ_y. Our signal, $I_x - I_z$ measures directly such a rotation. Any change in σ_y that is correlated with $\vec{\mathcal{E}}_s$ (for example, due to high voltage leakage currents), could result in a false Stark interference signal. Such optical rotation effects were suppressed in three ways. The probe beam laser was locked to the peak of the absorption line where the magnitude of optical rotation, which has a dispersive lineshape, should be close to zero. In addition, at the start of each data run, σ_y was made zero by small adjustments to B_y. Finally, by taking equal amounts of data in both $\hat{\epsilon}$ states, residual rotation signals should cancel because the Stark interference signal is the same for $\hat{\epsilon} = \hat{x} \pm \hat{z}$ while the optical rotation signal changes sign. As a result of these supressions, even if all of the measured high voltage leakage currents (≤ 0.1 nA) flowed in a path that maximized B_y, the resultant rotation signal would have been 1/30 of our final experimental error.

In the overnight data runs, the quadratic Stark shift (Stark splitting of the Rb energy levels) would give rise to a fractional change in absorptivity (quadratic in $\vec{\mathcal{E}}_s$ and linear in $\vec{\sigma}$) of average magnitude 25×10^{-8}. Although the voltage across the vapor cell was reversed to an accuracy of 0.1%, there was no guarantee that the electric field inside the cell reversed to this accuracy. If $\mathcal{E}_s^2$ were different for positive and negative voltages, then

TABLE I. Measured results.

Data set	Absorptivity $\alpha \pm 0.02$	Polarization $\sigma \pm 0.04$	$(a_{M1} + a_{E2})\vec{E}_s$ (units of 10^{-8}) $\hat{\epsilon} = \hat{x} + \hat{z}$	$(a_{M1} + a_{E2})\vec{E}_s$ (units of 10^{-8}) $\hat{\epsilon} = \hat{x} - \hat{z}$
1	1.07	0.83	10.1 ± 5.3	9.2 ± 2.9
2	1.15	0.77	15.6 ± 5.1	4.5 ± 4.5
3	1.22	0.79	9.0 ± 2.0	7.9 ± 2.9
4	1.07	0.60	3.4 ± 4.8	7.4 ± 4.6
5	1.18	0.62	7.4 ± 9.7	-1.7 ± 6.5
6	1.29	0.68	4.8 ± 4.0	9.7 ± 3.7
7	1.29	0.70	-0.1 ± 4.1	12.2 ± 3.9
8	1.36	0.65	5.2 ± 3.7	8.1 ± 3.9
9	1.25	0.65	9.1 ± 3.2	6.0 ± 2.7
Combined			7.2 ± 1.6	7.0 ± 1.4

the quadratic Stark shift signal would contain a component that appeared to be linear in $\vec{\mathcal{E}}_s$. By applying a small B_y field, it was found that the quadratic signal could be increased by a factor of 80 (to 2000×10^{-8}). During the day, shorter data runs were taken with $\pm B_y$ fields applied to search for signals linear in $\vec{\mathcal{E}}_s$ that arose from the large quadratic signals. The measured signal, linear in $\vec{\mathcal{E}}_s$, for these short runs had a typical magnitude of $(50 \pm 30) \times 10^{-8}$. A small correction for the quadratic Stark shift feedthrough was included in our final result, as described next.

RESULTS AND DISCUSSION

For each data set the four long and four short runs for a given direction of $\hat{\epsilon}$ were fit to the function:

$$S(\vec{\mathcal{E}}_s) = A + BS(\mathcal{E}_s^2) \tag{6}$$

and the fit parameter, A, was taken to be the desired Stark interference result. The uncertainty in A includes the statistical uncertainties of $S(\vec{\mathcal{E}}_s)$ and $S(\mathcal{E}_s^2)$, and the goodness of the fit. The results for $A = (a_{M1}+a_{E2})\mathcal{E}_s$ are given in Table I. Because a straight average over a complete set of vapor cell orientations best cancels a variety of potential systematic errors, we present our combined results in Table I as the unweighted average of each column and the error as the standard deviation of the mean. A comparison of the two columns reveals no indication of a signal arising from optical rotation, as discussed above. For our final result, we take the straight average of the combined results from each column. By repeating the analysis with no correction for the possible feedthrough of the quadratic Stark shift, that is, setting B in Eq. (6) equal to zero, we find that $S(\vec{\mathcal{E}}_s)$ is decreased by 6%. We combine this uncertainty in quadrature with the 10% uncertainty in the magnitude of $\vec{\mathcal{E}}_s$ to derive a systematic error that is 12% of the central value. Our result is then

$$a_{M1} + a_{E2} = (-2.37 \pm 0.37 \pm 0.28) \times 10^{-8}\ (\mathrm{kV/cm})^{-1}, \tag{7}$$

where the first error is statistical and the second is a systematic error.

Because the $M1$ contribution to the Stark interference is known with good accuracy from experimentally measured quantities [5] to be $a_{M1} = 2.45 \times 10^{-8}\ (\mathrm{kV/cm})^{-1}$, we can use our measurement to extract the $E2$ contribution. We find that

$$a_{E2} = (-4.82 \pm 0.47) \times 10^{-8}\ \ (\mathrm{kV/cm})^{-1}, \tag{8}$$

where we have combined the two errors in quadrature. The calculation of a_{E2} which depends on an infinite sum over atomic states requires detailed atomic theory. A simple central potential model for Rb atoms [5] has yielded a prediction for a_{E2} of $-4.6 \times 10^{-8}\ (\mathrm{kV/cm})^{-1}$, in good agreement with the measurement. A similar calculation for cesium atoms yields a tenfold larger result for $a_{E2}(\mathrm{Cs})$ due to the near degeneracy of the $6p$ and $5d$ atomic states, which would be interesting to test experimentally.

ACKNOWLEDGMENTS

We thank R. Morley for his expert fabrication of the vapor cells and S. K. Lamoreaux and P. Majumder for their helpful advice. This work was supported by the National Science Foundation under Grant No. PHY-9206408.

[1] M. A. Bouchiat and C. Bouchiat, J. Phys. (Paris) **36**, 493 (1975); M. A. Bouchiat *et al.*, Opt. Commun. **45**, 35 (1983).
[2] S. Chu, E. Cummins, and R. Conti, Phys. Lett. **60A**, 96 (1977).
[3] J. Hoffnagle *et al.*, Phys. Lett. **85A**, 143 (1981).
[4] S. L. Gilbert, R. N. Watts, and C. E. Wieman, Phys. Rev. A **27**, 581 (1983).
[5] J. Hodgdon, B. R. Heckel, and E. N. Fortson, Phys. Rev. A 43, 3343 (1991).
[6] S. K. Lamoreaux and E. N. Fortson, Phys. Rev. A 46, 7053 (1992).
[7] R. Marrus, D. McColm, and J. Yellin, Phys. Rev. **147**, 55 (1966).